Science of the Total Environment 906 (2024) 167660

Contents lists available at ScienceDirect

Science of the Total Environment

journal homepage: www.elsevier.com/locate/scitotenv

Electrochemical degradation of key drugs to treat COVID-19: Experimental analysis of the toxic by-products formation (PCDD/Fs)

Sophie Schröder, Inmaculada Ortiz, Ma.-Fresnedo San-Román *

Departamento de Ingenierías Química y Biomolecular, ETSIIyT, Universidad de Cantabria, Avda. de los Castros, 39005 Santander, Spain

HIGHLIGHTS

- Depollution of water containing different drugs: DEX, AMX, PAR and STR
- Finding of chlorophenols, hydroquinones and quinones as degradation intermediates
- PCDD/Fs congeners were determined, achieving concentrations up to 234.6 pg L^{-1}.
- Toxicity in terms of TEQ was analysed, reaching 30 pg L^{-1} for the DEX with NaCl case.

GRAPHICAL ABSTRACT

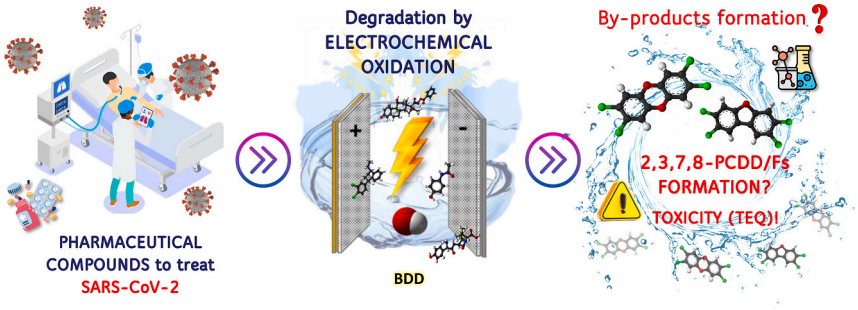

ARTICLE INFO

Editor: Paromita Chakraborty

Keywords:
Pharmaceutical compounds
COVID-19
Electrochemical oxidation
By-products and PCDD/Fs congeners
(toxicity) TEQ

ABSTRACT

Drug consumption has grown exponentially in recent decades, particularly during the COVID-19 pandemic, leading to their presence in various water sources. In this way, degradation technologies for pollutants, such as electrochemical oxidation (ELOX), have become crucial to safeguard the quality of natural resources. This study has as its starting point a previous research, which demonstrated the efficacy of ELOX in the removal of COVID-19 related-drugs, such as dexamethasone (DEX), paracetamol (PAR), amoxicillin (AMX), and sertraline (STR), using the electrolytes NaCl and Na_2SO_4. The present research aims to study the potential risks associated with the generation of toxic by-products, during the ELOX of cited drugs, specifically focusing on the highly chlorinated persistent organic pollutants (POPs), such as polychlorinated dibenzo-p-dioxins and dibenzofurans (PCDD/Fs). Dioxins and furans can be formed potentially in electrochemical systems from precursor molecules or non-precursor molecules in chloride medium. First, the degradation of the parent compounds was found to be complete. At this point, a comprehensive investigation was conducted to identify and analyse the by-products formed during the degradation process; precursors of PCDD/Fs, such as chlorophenols or hydroquinones were identified. Additionally, in continuation of the previous study, PCDD/Fs congeners were investigated, revealing elevated concentrations; the highest concentration obtained was for the congener 1,2,3,4,6,7,8-HpCDF (234.6 pg L^{-1} in NaCl) during degradation of the AMX. Finally, an assessment of the toxicity based on TEQ values was conducted, with DEX exhibiting the highest concentration among all compounds: 30.1 pg L^{-1} for NaCl medium. Therefore, the formation of minor by-products should not be underestimated, as they can significantly enhance the toxicity of the final sample, so the selection of the appropriate remediation technology, as well as the

* Corresponding author.
E-mail address: sanromm@unican.es (Ma.-F. San-Román).

https://doi.org/10.1016/j.scitotenv.2023.167660
Received 21 July 2023; Received in revised form 5 October 2023; Accepted 5 October 2023
Available online 7 October 2023

optimization of experimental operating variables, is determining in the treatment of pharmaceutical-contaminated waters.

1. Introduction

Pharmaceutical and personal care products (PPCPs) are part of the Emerging Contaminants group (ECs). Among them, drugs are found, whose consumption has continuously increased, especially in the case of some of them, as a consequence of the COVID-19 pandemic (WHO and UNICEF, 2020), generating elevated concentrations in aquatic environments, from ng L^{-1} to mg L^{-1} (Hawash et al., 2023; Pariente et al., 2022; Rapp-Wright et al., 2023). These concentration levels are considered harmful to aquatic organisms and consequently, human beings (Abajo et al., 2023; Korkmaz et al., 2023). PPCPs are particularly persistent compared to other organic contaminants. They enter the environment through hospital wastewater, pharmaceutical industries, wastewater treatment plants (WWTPs), etc., appearing as degradation by-products (Hawash et al., 2023; Kumar et al., 2023; Yan et al., 2023).

Among the pharmaceutical compounds employed in combating the symptoms of the SARS-CoV-2 virus, it can be found the dexamethasone (DEX), a common anti-inflammatory and immunosuppressive glucocorticoid (Musee et al., 2021), the amoxicillin (AMX), an antibiotic drug commonly used to treat bacterial infections, such as chest infections, including pneumonia, and the paracetamol (PAR), a painkiller utilized to alleviate primary symptoms, such as fever or headache (Morales-Paredes et al., 2022; Zhu et al., 2021). The psychiatric drugs like sertraline (STR), a SSRI (selective serotonin reuptake inhibitor) antidepressant, were used during the pandemic to treat anxiety and depression, which was reflected in a higher consumption, generating higher concentrations in water compared to non-pandemic periods (Diaz-Camal et al., 2022; Rabeea et al., 2021).

Currently, WWTPs are not efficient enough with their common treatments to eliminate these types of compounds. It has been found kind of elevated concentrations of pharmaceutical compounds in several WWTPs influents, as acetaminophen (2282 μg L^{-1}) (Alharbi et al., 2023), or in effluents, such as carbamazepine (0.28–0.51 μg L^{-1}), ofloxacin (<0.05–0.18 μg L^{-1}) (Äystö et al., 2023) or hydrochlorothiazide (1067 ng L^{-1}) (Rapp-Wright et al., 2023), among others. In the case of wastewaters, Pariente et al. (2022) gathered different concentrations of some drugs in a review work, such as paracetamol, amoxicillin, or levofloxacin, found in concentrations up to 1.3, 4 and 1.1 mg L^{-1}, respectively. Added to this, it has been reported that the lack of legislation in some countries of southern Asia, such as India, Vietnam or Pakistan, among others, increases this problem, due to the direct release into the environment of pharmaceuticals processes waters without previous treatment, which contain high concentrations of drugs (Patel et al., 2019). So, for example, up to 141 mg L^{-1} of the anti-inflammatory ofloxacin were reached along the Yamuna River in Delhi (India) (Akhter et al., 2023), or in a lesser amount, 6 mg L^{-1} of the antibiotic norfloxacin, in Vietnam (Binh et al., 2018).

In this context, advanced oxidation processes (AOPs) are viable options for treating drugs, among other ECs. Within AOPs, electrochemical oxidation, ELOX, is widely employed and successfully proved in remediating such solutions, due to the generation of •OH radicals, powerful and non-selective oxidizing agents (Schröder et al., 2023). However, the literature describes studies in which the electrochemical oxidation of the main compound can give rise to intermediate by-products that can be formed unintentionally, due to the incomplete mineralization of the parent compounds. Regarding DEX, the studies that have been found are mostly focused on the degradation of the parent compound, scarcely tackling the formation of by-products, and mainly applying photolytic/photocatalytic treatments (Cantalupi et al., 2020; Ghenaatgar et al., 2019; Guo et al., 2017; Markic et al., 2018; Pretali et al., 2021; Rasolevandi et al., 2019). Just a recent work applied electrochemical oxidation using a BDD (boron doped diamond) anode (Grilla et al., 2021). Prednisolone, along with several variations of the dexamethasone molecule or hydroxylated dexamethasone, have been identified as one of the most detected by-products during the degradation process (Grilla et al., 2021; Guo et al., 2017; Quaresma et al., 2021; Rasolevandi et al., 2019). Conversely, the AMX and PAR electrochemical oxidation has been further studied, detecting by-products such as hydroxylated compounds, hydroquinone, benzoquinone, and chlorinated molecular structures of the parent compound (Ganiyu et al., 2019, 2016; Le et al., 2017; Liu et al., 2019; Olvera-Vargas et al., 2018; Waterston et al., 2006; Zhang et al., 2018). In the case of STR, there are very few studies that analyse the by-products formed from its degradation. 3,4-dichlorophenol, and mono-, di-, or tri-hydroxylated STR were identified after the application of photo-transformation technologies (Calza et al., 2021; Gornik et al., 2020; Jiménez-Holgado et al., 2021). Furthermore, beyond AOPs, alternative technologies such as bioremediation using microorganisms, adsorption with materials like activated carbon, and membrane filtration (such as nanofiltration and reverse osmosis) are emerging for drugs' degradation (Al-sareji et al., 2023; Angeles-de Paz et al., 2023; Arun et al., 2023; Moghaddam et al., 2023).

The literature highlights that the by-products generated during organic pollutant oxidation can be potentially more dangerous than the initial compounds themselves such as polychlorinated dibenzo-p-dioxins and furans, mostly known as dioxins and furans (PCDD/Fs), highlighting, especially, 17 of the 210 PCDD/Fs congeners due to their associated elevated toxicity, caused by the chlorine atoms in at least, positions 2, 3, 7 and 8. These compounds are formed from different molecules that act as precursor compounds, and also they can be formed from non-precursor compounds in chloride presence, such as the aromatic organic compounds (Schröder et al., 2023, 2020; Solá-Gutiérrez et al., 2018; Vallejo et al., 2014).

This research has as its starting point the acquired knowledge from a prior study by Schröder et al. (2023), which focused on the electrochemical degradation of DEX, AMX, PAR, and STR, and examined the formation of PCDD/Fs in terms of homologue groups. This current research represents a significant advancement in the investigation field by conducting a more comprehensive analysis. Firstly, an in-depth examination of the intermediate by-products formed during the ELOX of highly concentrated solutions of the COVID-19 related drugs was carried out using a GC–MS, with a special focus in the precursor compounds of dioxins and furans. Next, the analysis of the PCDD/F congeners was performed. Finally, the equivalent toxicity (TEQ) assessment was conducted aiming to know the potential harm that can reach the treated wastewater, containing drugs, when ELOX is applied. This study aims to contribute to the limited knowledge available regarding the degradation of these types of compounds when using AOPs, which will allow to act accordingly to avoid the final toxicity of treated samples.

2. Materials and methods

2.1. Chemicals

Dexamethasone (≥98 %) (CAS: 50-02-2) (DEX), amoxicillin trihydrate (≥95 %) (CAS: 61336-70-7) (AMX) and paracetamol (acetaminophen) (≥99 %) (CAS: 103-90-2) (PAR) were purchased from Sigma-Aldrich, and sertraline hydrochloride (≥98 %) (CAS: 79559-97-0) (STR) was from TCI. For the HPLC analysis, acetonitrile LiChrosolv® (≥99.9 %) from Merck and laboratory-prepared phosphate buffer were employed. EPA 1613 standard solutions from Wellington Laboratories were employed (CS-1 to CS-5, LCS and ISS) to calibrate the equipment, the recovery and quantification of PCDD/Fs and quality control. Toluene

Suprasolv®, dichloromethane UniSolv®, n-hexane UniSolv®, acetone Suprasolv®, sulfuric acid Normapur® and sodium sulfate (Emsure®) were acquired from Merck. Solid sorbents (silica, alumina and activated carbon chromatography columns) from Technospec were employed in the purification of PCDD/Fs samples through EPA 1613 method. Two different types of syringe filters, 1 μm APFB (Merck Millipore) and 0.45 μm Millex (Millipore), were employed, as well as a 2.7 μm glass microfiber filter (Whatman). The solutions were prepared with deionized ultrapure Milli-Q-Water (resistivity = 18.2 MΩ·cm) purified with Milli-Q device (Millipore).

2.2. Electrochemical experiments

Solutions (2 L) containing different initial concentrations of the correspondent drug were electrochemically treated in medium/high power laboratory-scale electrochemical plant (APRIA Systems S.L.). This plant possesses a jacketed mixing tank (1 L) and an electrochemical cell of two rectangular electrodes of 210 cm^2 of anodic area (anode of Nb/BDD and AISI316 stainless steel as cathode) and an electrode gap of 2 mm. A plant scheme can be found in a previous work (Schröder et al., 2023). The operational flow rate was 300 L h^{-1} and the supporting electrolytes employed were NaCl (56.3 mM) and Na_2SO_4 in combination with NaCl (21.1 mM + 2.8 mM, respectively) to reach the necessary conductivity value (7.5 mS cm^{-1}) to operate with the electrochemical cell. 2.8 mM of NaCl was selected with the aim to simulate the equivalent amount of the common chlorine (Cl^-) content in WWTP effluents, around 100 mg L^{-1} (measured for this work in a real effluent). The initial concentrations were 80 mg L^{-1} for DEX (0.2 mM), and 3000 mg L^{-1} for AMX (7.1 mM), PAR (19.8 mM) and STR (8.7 mM), and correspondingly, the current density (J) applied was 48 A m^{-2} for DEX, 1000 A m^{-2} for AMX and PAR and 900 A m^{-2} for STR (limiting current density, J_{lim}: 25.7 A m^{-2} for DEX; 960 A m^{-2} for AMX; 963 A m^{-2} for PAR and 851 A m^{-2} for STR). These current density (J) values were selected to work under mass-transport control ($J > J_{lim}$). The calculations carried out to obtain these J_{lim} values are detailed in the Supplementary material, where Table S1 details the J values for all the experiments. The experiments were conducted in batch mode and two replicates were carried out.

2.3. Chemical analysis

The four studied drugs (DEX, AMX, PAR and STR) were quantified in an Agilent Series 1100 HPLC chromatograph, equipped with an Agilent ZORBAX 80 Å Extend-C18 5 μm column (3.0 × 150 mm) and a photodiode array (PDA) 1260 detector. The analytical method employed for each of the analysed drugs (DEX, AMX, PAR, and STR) was described thoroughly in a previous publication (Schröder et al., 2023). Compounds were confirmed by using authentic standards, matching their retention times and absorbance spectra.

Qualitative analysis of the by-products formed during the ELOX of drugs was carried out in gas chromatography–mass spectrometry (GC–MS). Prior to the GC–MS analysis, a concentration stage was performed. To this, for the DEX case, 100 mL of initial sample were added to a 500 mL separatory funnel and extracted four times with 20 mL of dichloromethane (each time). Then the organic extract was concentrated twice in a rotary evaporator, and after that, a N_2 stream. For the rest of the drugs (AMX, PAR and STR), aliquots of samples were taken at different oxidation times (30 mL) and extracted two times with 20 mL of dichloromethane using a 100 mL separatory funnel. Then, all samples were evaporated at the same time in a TurboVap® LV evaporator, for 3 h until a volume of ≈1 mL; and finally, transferred to amber vials for further analysis in GC–MS. A Shimadzu QP2010 Ultra apparatus equipped with an autosampler was used, with an HP-5MS column (30 m × 0.25 mm × 0.1 mm) from Agilent. The mass spectrometer was operated in the electron impact ionization mode (70 eV) and data acquisition was in full scan mode (range: m/z 35–400). The analytical method used was different for each drug studied, which is detailed in Table S2 of the Supplementary material. The identification of the by-products involved a meticulous procedure that entailed a comprehensive comparison of their respective mass spectra against the spectral profiles contained within the NIST08 database. A match percentage was derived through the comparison of the mass spectra and characteristic ions and fragments of a specific peak with those exhibited by a known compound from the reference library (Tables S3–S6 of the SM) (US EPA, 2007, 1998). To ensure the accuracy and reliability of the identification process, a predefined threshold was set at a match percentage exceeding 70 %, after which the compound was deemed identified (Gary Mallard and Reed, 1997). Additionally, the mass abundancies were also compared, in order to avoid misinterpretations of the compound identification.

The PCDD/Fs samples analysis followed the EPA 1613 method (US EPA 1613, 1994). The detailed process can be found in a previous work (Schröder et al., 2023). The PCDD/Fs samples were analysed and quantified also by the Chromatography Service of the University of Cantabria (SERCROM). In order to guarantee the analysis of the PCDD/Fs, two standard solutions have been employed: 1613 LCS, a solution/mixture of fifteen $^{13}C_{12}$-labelled chlorinated dibenzo-p-dioxins (2,3,7,8-$^{13}C_{12}$-PCDDs) and dibenzofurans (2,3,7,8-$^{13}C_{12}$-PCDFs) utilized to calculate the recoveries of the labelled compounds obtained through the various stages followed to prepare the sample before the analysis; and ISS, an internal standard, which is added to the sample previous to the chromatographic analysis, to calculate the concentrations of the labelled compounds (1,2,3,4-TCDD $^{13}C_{12}$ and 1,2,3,7,8,9-HxCDD $^{13}C_{12}$) and the OCDF. EPA 1613 CLS-CS4 has been utilized as calibration standard solution. For further consultation, in Tables S7-S9 of the Supplementary material, are gathered the concentrations of the 1613 ICS, ISS and CLS-CL4 standards employed. The isotopic dilution method was applied to conduct the quantitative determination of the PCDD/Fs. Relative response factors (RRFs), acquired from the calibration curve by the analysis of 1613CSL and 1613CS-1–CS-4 standard solution mixtures for tetra- to octa-PCDD/Fs were used to determine the dioxins and furans concentration in the samples. The recoveries of the labelled standards were calculated by the use of a combination of two labelled PCDD/Fs (contained within the ISS).

Finally, it is of the utmost importance to guarantee the accuracy of the method, as well as the recoveries and the absence of contamination during the analysis. It was proven, on the one hand, that the recoveries of the samples were within the ranges established by the US EPA method (30–100 %), and on the other hand, blank assays were performed, covering the whole sample preparation process, with ultrapure water spiked with LCS standard. These blanks' analysis showed that PCDD/Fs were present in negligible concentrations, showing the near absence of contamination, and in addition, these blanks were subtracted from the detected PCDD/Fs concentrations for each performed experiment, in order to ensure the reliability of the results obtained. All the recovery values are detailed in Tables S10-S12 of the Supplementary material, along with the calibration curves for the 17 PCDD/Fs congeners, Fig. S1a–q. The average detection limits (LOD) were within the range of 0.01–0.85 pg L^{-1} for all the analysis; and the average quantification limits (LOQ) were within the range of 0.19–2.09 pg L^{-1}.

3. Results and discussion

3.1. Electrochemical oxidation of drugs around the solubility limit

The degradation of highly concentrated solutions was carried out in order to detect the largest number of reaction by-products formed during the electrochemical oxidation process; 80 mg L^{-1} of DEX (0.2 mM) and 3000 mg L^{-1} of AMX, PAR and STR (7.1, 19.8 and 8.7 mM, respectively). These concentrations were selected depending on the compound solubility limit. In the case of PAR, the solubility limit is 14,000 mg L^{-1}, but 3000 mg L^{-1} was set for all the compounds to work under the same conditions. The results of the electrooxidation of each

drug for both electrolytic media are depicted in Fig. 1. The complete degradation for AMX, PAR and STR in NaCl medium required a specific electrical charge (Q) below 10 A h L^{-1}, and around 3 A h L^{-1} for DEX. This difference is due to the initial concentration used, 80 mg L^{-1} for DEX versus 3000 mg L^{-1} used for AMX, PAR and STR (see the calculations in the Supplementary material). 8, 12, 20, and 50 min were needed, to reach 50 % of STR, AMX, PAR and DEX degradation, respectively (blue lines).

In the electrolytic medium Na_2SO_4 + NaCl, the experiments were slower regarding NaCl medium: around 15, 20, 30, and 50 min were employed to reach 50 % of degradation, for STR, AMX, PAR and DEX, respectively (red lines). As can be observed in the kinetics and in the molecule represented in Fig. 1a, the DEX degradation is independent of the electrolytic medium. This fact can be due to the complexity and robustness of the DEX molecule, which seems to need species oxidizing highly for its degradation, being probably the hydroxyl radicals (•OH), existing in both electrolytic media, those that contribute more to its elimination, given its elevated production from water, high oxidation potential and non-selective oxidation (Schröder et al., 2023). The rest of the studied molecules possess some weak bonds, easy to break under the applied conditions, as has been corroborated by its fast degradation in comparison with DEX.

For both electrolytic mediums, the degradation order follows the same trend STR > AMX > PAR > DEX. The corresponding experimental error is depicted in each degradation curve.

Finally, the analysis of the degradation of all studied cases was carried out fitting the data a pseudo-first-order kinetics (represented in Fig. S2 of the Supplementary material). In Table S13 (Supplementary material), the kinetic constants for both types of experiments are detailed. The range of the pseudo-first-order rate constants for DEX, PAR, and AMX under all operating conditions is found to be between 1.1 · 10^{-2} and 5.1 · 10^{-2} min^{-1} for both electrolytic media. However, for STR, the range is an order of magnitude higher, between 4.0 · 10^{-2} and 1.0 · 10^{-1} min^{-1}; with the higher value corresponding to NaCl medium and the lower value, Na_2SO_4 + NaCl medium. The obtained kinetics confirmed the proposed tendencies in this work, and in a previous study of our research group (Schröder et al., 2023) when a lesser concentration of each drug (10 mg L^{-1}) and two electrolytic media were used; the rate of degradation is a function of the bonds type in the molecule and their difficulty in breaking.

3.2. Analysis of the degradation intermediates and toxicity

3.2.1. Identification of electro-oxidation intermediates: kinetic analysis

In the literature, it has been reported that the pharmaceuticals under study in this research can generate by-products during their degradation, such as hydroquinones, benzoquinones, or chlorophenols, among others (Siciliano et al., 2021), due to their interaction with the oxidizing radicals of the medium; •OH radicals produced in the BDD anode or radicals formed from the electrolyte added to the samples, NaCl and Na_2SO_4. In this direction, when electro-oxidation technology is applied, the radicals that are formed mostly in terms of quantity and oxidative power are •OH radicals (E^0 (•OH/H_2O)= 2.73 V), Cl• (E^0(Cl•/Cl^-)= 2.43 V); Cl_2^- (E^0(Cl_2•$^-$/2Cl^-)= 2.13 V) and E^0($SO_4^{\bullet-}$/SO_4^{2-})= 2.43 V (Schröder et al., 2023). To clarify, on the one hand, the electro-oxidation experiments ended when the parent compound was completely degraded. On the other hand, elevated concentrations of each drug were selected in order to make a "zoom in" on the processes occurring at a minimum scale. This approach was taken in order to avoid issues associated with detection limits and experimental errors that involve the formed by-

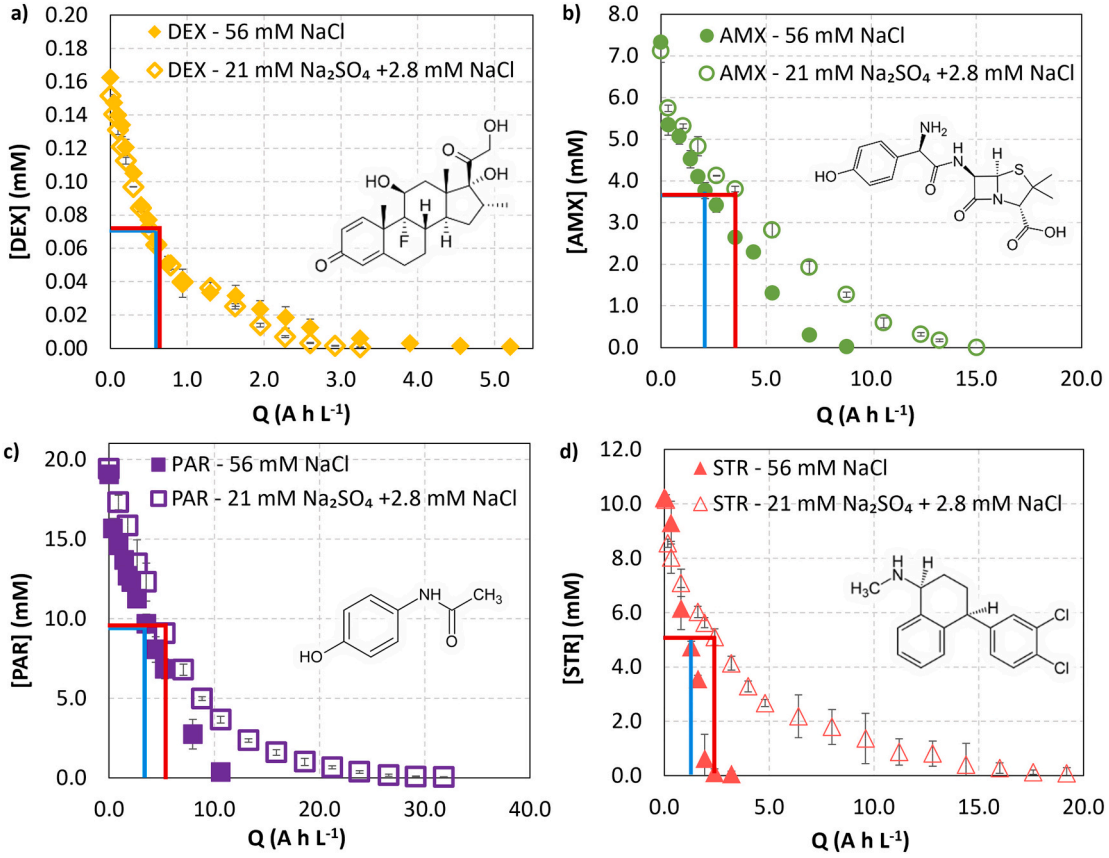

Fig. 1. Degradation of the COVID-19 drugs with the specific electrical charge: a) DEX (yellow diamonds), b) AMX (green circles), c) PAR (purple squares) and d) STR (pink triangles); with $[DEX]_0$= 80 mg L^{-1} and $[AMX]_0$=$[PAR]_0$=$[STR]_0$= 3000 mg L^{-1}. Blue and red lines represent the time needed to degrade 50 % of each drug for NaCl and Na_2SO_4 + NaCl electrolytic medium, respectively.

products, when pollutants to be degraded are found at low concentrations. Knowing the formed by-products, it is possible to understand the PCDD/Fs mechanism formation and act accordingly to avoid the final toxicity of the treated samples. Taking into account the results obtained in previous studies by the authors (Schröder et al., 2023; Solá-Gutiérrez et al., 2018, 2019), working with other PPCPs (triclosan), it is assumed that similar behaviour could be observed. In these works, it has verified the qualitatively proportional formation of by-products as the initial concentration of the pollutant increased (Schröder et al., 2023; Solá-Gutiérrez et al., 2018, 2019). TCS studied concentrations were between 10 and 150 mg L^{-1}. After degradation, the analysis of the by-products formed was carried out, finding PCDD/Fs precursors, such as 2,4-dichlorophenol, 4-chlorocatechol, 2-chlorohydroquinone, 2-chloro-4-methoxyphenol and 1-chloro-2,5-dimethoxybenzene; or non-chlorinated compounds (but PCDD/Fs precursors in chloride presence) like 2-ethyl-hexanol and diphenyl ether benzene, for each study case. In the same way, PCDD/Fs concentrations of 411, 34,178 and 163,319 pg L^{-1} were obtained for 10, 100 and 150 mg L^{-1} of TCS, respectively.

Different by-products were detected for each studied drug, which are described hereunder. The selection of the compounds was carried out considering the compounds formed in a higher amount, i.e., visible and defined peaks, with the highest area, and that fulfils the criteria detailed in Section 2.3. Additionally, Tables S3–S6 of the Supplementary material display the rest of the identified by-products, which were present in a lesser concentration, for all the studied drugs next to their retention time (RT) and their main fragments (m/z) for both electrolytic media. These tables also show all the chemical structures of each detected molecule.

The main degradation pathways for DEX have been studied principally in photo-assisted technologies, and just one recent work (Grilla et al., 2021) analysed the by-products generated after an electroremediation process employing a BDD anode. This study provides an advance in knowledge in regard to the detection of the generated by-products during the ELOX with BDD of DEX using NaCl as electrolyte, due to, until now, according to recent literature, some of them have not been identified in previous works. Among these by-products, several have not been detected in previous studies. As it is described in the literature and it is shown in Fig. 2a, the DEX degradation pathway may comprise one or more of the steps described hereafter: i) loss of the fluorine atom, such has happened in all the detected molecules in this work (Fig. 2b and c), ii) transformation and/or loss of -CO-CH_2OH group in the molecules MTT, DHT and MDEO (Na_2SO_4 + NaCl medium) (Fig. 2c), and finally, iii) ring opening, typically happening after previous the pathways have occurred, as in the case of PTCP, PTN, 2,4-DCP and NAP (Fig. 2b) and MDOD (Fig. 2c) (Babu et al., 2009; Calza et al., 2001; Cantalupi et al., 2020; Guo et al., 2017; Pazoki et al., 2016; Pretali et al., 2021; Quaresma et al., 2021; Rasolevandi et al., 2019; Sulaiman et al., 2014). It is worth highlighting that the compounds such as BCM and NAP (Fig. 2b) and MTT, DHT and MDOD (Fig. 2c) are known as DEX-alike compounds, because they are DEX molecules slightly modified, or fragments of DEX, generated during the oxidation process.

From a kinetic point of view, the intermediates of the degradation DEX in NaCl medium (Fig. 2b) show the same tendency, they grow till a maximum, and then they decrease until practically zero values, except for PTCP and PTN, which still has concentration at the final time. In this sense, there are indications that PCTP can originate from the modification and combination of chlorophenols (for example, 2,4-DCP) (Fernández-Castro et al., 2016) that are partially transformed into furans, as shown in the experimental study results of the PCDD/Fs analysis carried out in this study (Section 3.3) (Fernández-Castro et al., 2016;

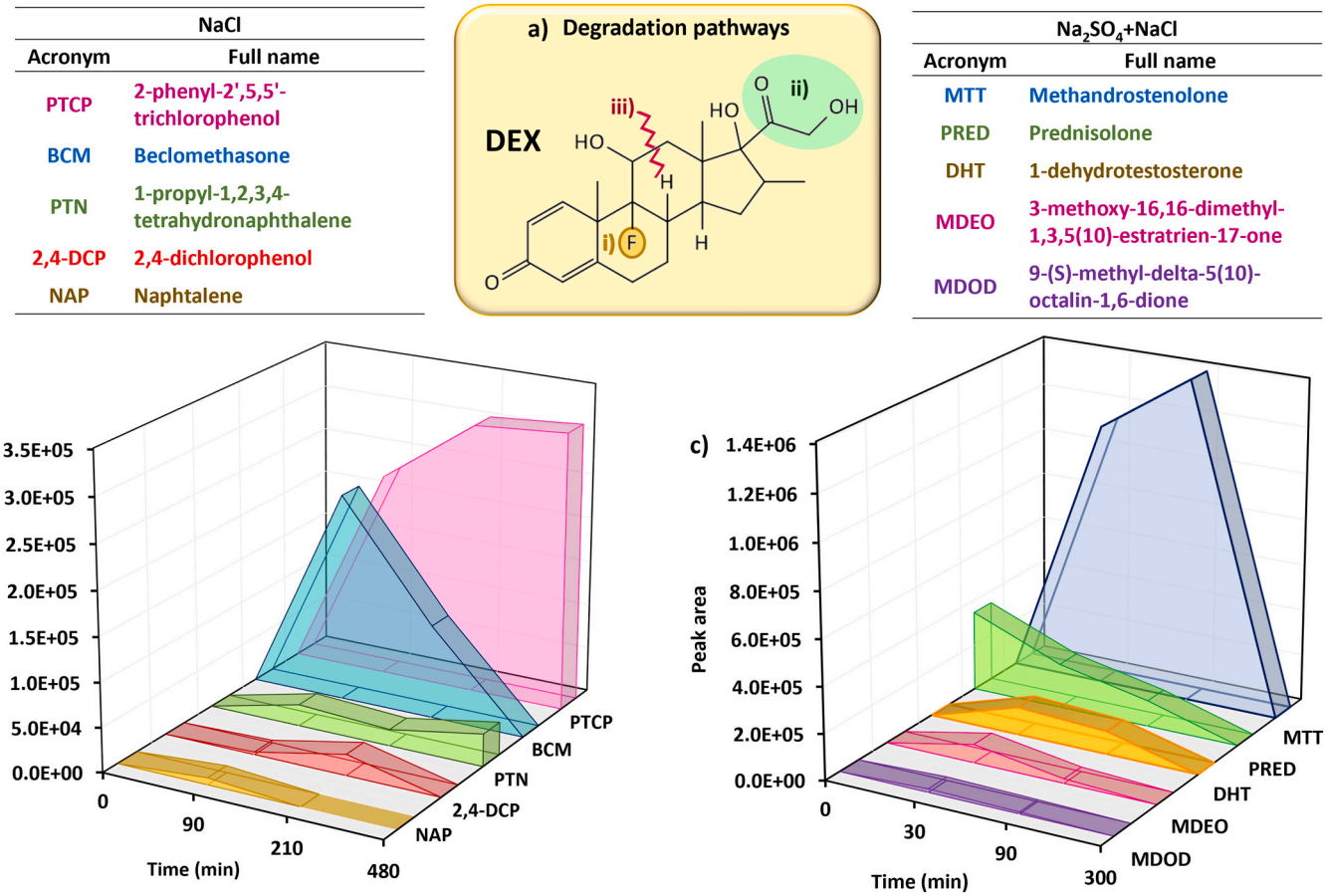

Fig. 2. Kinetics of the by-products identified during DEX degradation, a) main pathways, b) electrolyte: NaCl and c) electrolyte: Na_2SO_4 + NaCl.

Schröder et al., 2023). Regarding the PTN, it is not completely eliminated; it is a molecule similar to polycyclic aromatic hydrocarbons (PAHs), whose electrochemical degradation is specifically influenced by its structure, for example, pyrene degrades more quickly than phenanthrene, despite having a higher molecular weight, because it has inaccessible carbon sites to hydroxyl radicals (Rajasekhara et al., 2021). PTCP is the compound formed with higher concentration, maximum at final time (480 min), with a peak area of $3.1 \cdot 10^5$. This compound is followed by beclomethasone (BCM) (similar molecule to dexamethasone but with a chlorine atom on it) reaching a maximum at 90 min with a peak area of $\approx 10^5$. A highlight, the PCDD/Fs precursor, 2,4-dichlorophenol, reached a maximum concentration at 210 min, with a peak area in the order of $\approx 10^4$. For the electrolytic medium Na_2SO_4 + NaCl (Fig. 2c), all the compounds, except PRED, follow the same trend as for the NaCl medium, increasing up to a maximum and decreasing until zero values. The greatest concentration corresponded to methandrostenolone (MTT), which reached its maximum point at 90 min (peak area $\approx 10^6$), and subsequently decreased until practically its disappearance at the end of the experiment. It can be appreciated that prednisolone (PRED) is detected at the initial time, which could be an impurity of DEX original dissolution, due to the similarity of the molecule shape (steroid shape). The rest of the compounds, DHT and MDOD, are formed in lesser amounts, in the order of 10^4–10^5 (peak area), with maximum points at 30 min. It is noticeable that possible fragments of the dexamethasone degradation, PTN, NAP (Fig. 2b) and MDOD (Fig. 2c), as well as some dexamethasone-like compounds (DHT) (Fig. 2c), are formed in lower amounts, which allows understanding the difficulty of carrying out the degradation of the parent compound. In general terms, the rest of the detected by-products reach zero values at the end of the experiment, due to the presence of weak bonds, which can be easily cleaved, and therefore, achieve a rapid degradation.

For the AMX case, various studies analysed different by-products formed during the ELOX process, but just one was using a BDD anode (Frontistis et al., 2017). This study takes a step further and examines the degradation intermediates generated at a BDD anode in two different electrolytic media, which include a series of chlorophenols and other chlorinated compounds, such as chlorophenols, chlorohydroquinones or hydroquinones (Fig. 3). The formation of the by-products is described hereunder through the different AMX rupture pathways gathered from the literature and shown in Fig. 3a: i) break of different bonds of the molecule forming fragments like DMD or 4-NC (Fig. 3c) (Farhat et al., 2015; Frontistis et al., 2017; Ganiyu et al., 2016; Saha et al., 2022), ii) on the one hand, the opening of the β-lactam ring can occur, and on the other hand, hydroxylation, dehydrogenation and/or chlorination reactions on the phenolic ring, forming 2,4,5-TCP, Cl-HQ, 2,5-DCHQ, HQ, 4-CP, 2,4-DCP and Cl-BQ, (Fig. 3b and c) (Ferreira et al., 2020; Frontistis et al., 2017; Ganiyu et al., 2016; Tan et al., 2020); and finally iii) the chlorination of the phenolic ring due to the action of the chlorine radicals (Lei et al., 2019) generating 2,4,5-TCP, Cl-HQ, 4-CP and 2,4-DCP (Fig. 3b); 3,4-DBA and PTCP (Fig. 3c). The formation of these type of by-products is relatively easy due to the weak bonds present in the AMX structure, which is consistent with its rapid degradation.

Regarding its kinetic behaviour, for the NaCl experiments (Fig. 3b), all the compounds follow the same tendency, increasing with time, until reaching the highest values at the end of the experiment, which may be because to that the total degradation, or their transformation in PCDD/Fs, requires experimental times longer than 50 min, as it has been proven in other study cases (Schröder et al., 2021). For example, HQ needs 85 min to degrade in NaCl+Na_2SO_4 medium (Fig. 3c). The by-product with major concentration (peak area) was 2,4,5-dichlorophenol (2,4,5-TCP), with a peak area of $2.1 \cdot 10^6$ at 50 min, when there is no AMX in the solution. Next, the Cl-HQ appears as the second by-product formed with a peak area $1.6 \cdot 10^6$ at 50 min. The rest of the compounds have a peak area lower than $5.0 \cdot 10^5$ (2,5-DCHQ, HQ, 4-CP, 2,4-DCP

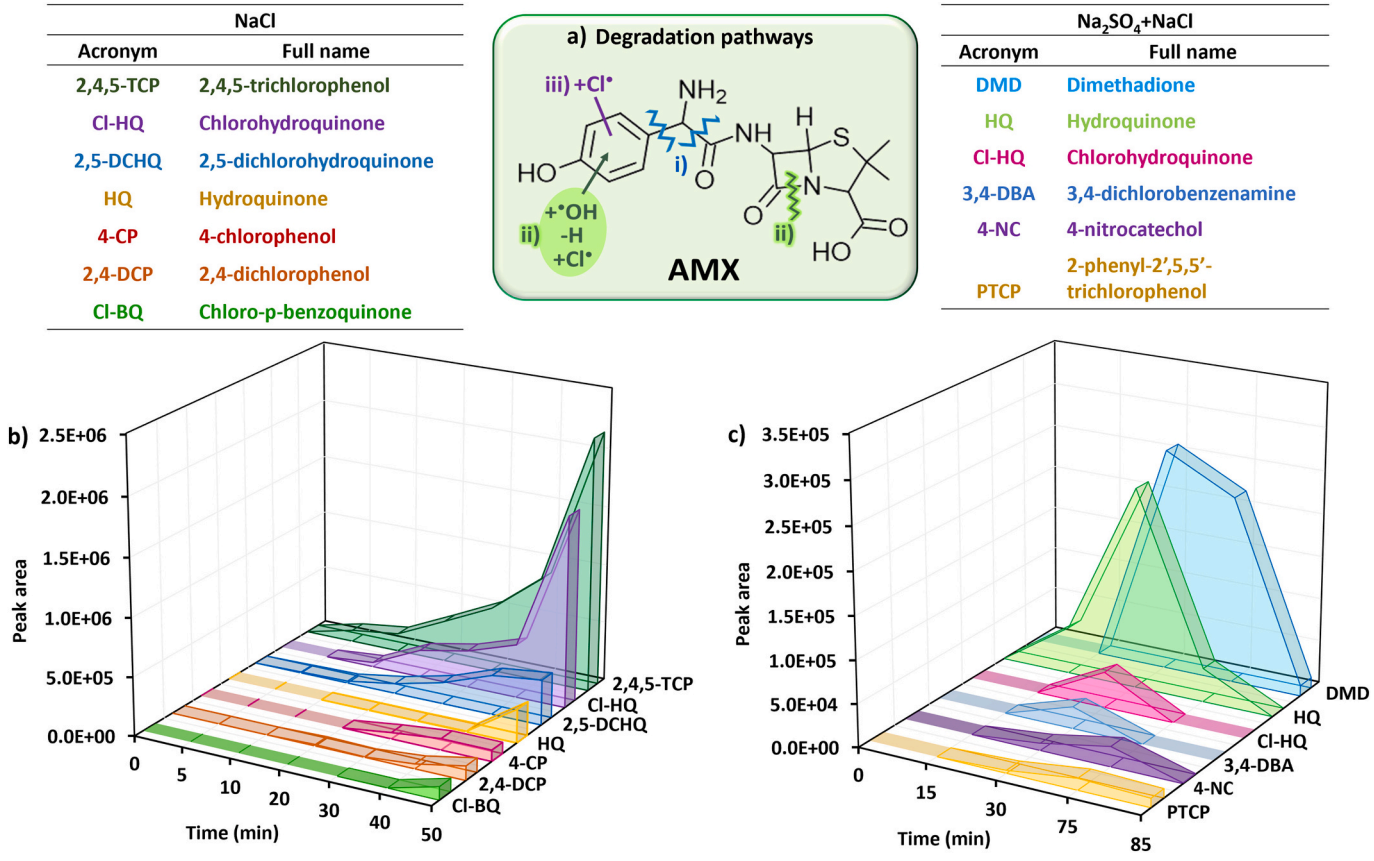

Fig. 3. Kinetics of the by-products identified during AMX degradation, a) main pathways, b) electrolyte: NaCl and c) electrolyte: Na_2SO_4 + NaCl.

and Cl-BQ) (Fig. 3b). Conversely, for the combined electrolyte medium, Na_2SO_4 + NaCl (Fig. 3c), the evolution of the by-products follows a different tendency that in NaCl case, all increase with time until a maximum, and nearly all by-products end in negligible concentrations (Fig. 3c). The slower degradation of the AMX (85 min), allows that the formed by-products are being degraded along with the original compound, resulting in its almost complete disappearance. DMD is the compound formed in the greatest amount, followed by HQ, with area values in the order of 2–2.5 · 10^5. Then, the Cl-HQ and 3,4-DBA, which have the highest point at 30 min (values among 2.3–2.6 · 10^5).

Next, based on the criteria established for compound identification by gas chromatography, Fig. 4 provides a detailed overview of the principal by-products detected during the ELOX of PAR, employing both NaCl and NaCl+Na_2SO_4 as electrolytes. Several studies have been conducted employing ELOX for the remediation of PAR-containing solutions, in various electrolytic media and using different anode materials (De Luna et al., 2012; Ganiyu et al., 2019; Ghanbari et al., 2021; Le et al., 2017; Liu et al., 2019; Olvera-Vargas et al., 2018; Periyasamy and Muthuchamy, 2018; Sun et al., 2018; Zhang et al., 2018). However, this research makes a significant contribution to the current state of knowledge by detecting multiple chlorophenols, not identified recently in the literature, during the ELOX process using two different electrolytes, particularly, with Na_2SO_4 + NaCl. Almost, all the detected by-products are kind of benzene molecules, because of the PAR molecular shape, which permits the breakage of some bonds, generating directly these kinds of compounds in an easy way, which is corroborated by its fast elimination. The main degradation pathways of the paracetamol molecule, according to the available literature, are four, which are shown in Fig. 4a: i) first, the •OH radicals favour the attack at the para-position with respect to the •OH functional group of the phenolic ring, forming HQ and BQ (Fig. 4b); ii) •OH radicals can attack the peptide bond, generating 4-NP (Fig. 4b); iii) different hydroxylated paracetamol molecules can be formed, when •OH radicals attack to other positions of the phenolic ring, like 4-NC and 1,3-BDO (Fig. 4c); iv) sometimes when the oxidation takes place in presence of chlorine (Cl^-), different chlorinated by-products can be formed, such as NHPA (chlorinated paracetamol), Cl-BQ, Cl-HQ, 2,5-DCBQ, 2,5-DCHQ and 2,4,5-TCP (Fig. 4b); 3,4-DCP and 3,4-DBA (Fig. 4c), due to their interaction with the chlorine radicals formed ($Cl^•$ and $Cl_2^{-•}$) (De Luna et al., 2012; Farhat et al., 2015; Ganiyu et al., 2019; Ghanbari et al., 2021; Le et al., 2017; Liu et al., 2019; Olvera-Vargas et al., 2018; Periyasamy and Muthuchamy, 2018; Saha et al., 2022; Sun et al., 2018; Zhang et al., 2018).

The kinetics of the detected intermediates have been represented in Fig. 4b (NaCl medium) and Fig. 4c (Na_2SO_4 + NaCl medium). For the NaCl case, some compounds follow the same tendency, growing up to reach a maximum at 45 min and decreasing to low concentration values: NHPA, 4-NP, Cl-HQ, HQ and BQ; and other ones which reached their maximum at the final experimental time: Cl-BQ, 2,5-DCBQ, 2,5-DCHQ and 2,4,5-TCP (60 min). The compound formed in the greatest amount was NHPA (a chlorinated paracetamol molecule), which achieved the greatest value at 45 min (2.7 · 10^6 peak area). As previously mentioned, this compound is a PAR molecule with a chlorine atom added in the phenolic ring, undergoing continuous and steady formation until its maximum, coinciding with the peak of most of the other by-products. It eventually degrades into other compounds, which may explain the increased concentration of Cl-BQ, Cl-HQ, and 2,5-DCBQ at the final time of the experiment. The higher concentration of NHPA can be attributed to its easy formation, due to the significant amount of chlorine atoms present in the medium. Then, in order of concentrations, appears Cl-BQ, followed by Cl-HQ, HQ, BQ, 2,5-DCBQ, 2,5-DCHQ and 2,4,5-TCP, with peak area values in their higher points between 9.3 · 10^6 and 1.1 · 10^5 (between 45 and 60 min) On the other hand, for the other electrolyte medium (Na_2SO_4 + NaCl) (Fig. 4c), concentrations all are increased until 60 min (highest point), decreasing until values close to zero. This is similar to the case of AMX with Na_2SO_4 + NaCl; it takes approximately three times longer to degrade the parent compound, and, therefore, the

NaCl	
Acronym	Full name
NHPA	N-(3-Chloro-4-hydroxyphenyl)acetamide
4-NP	4-nitrophenol
Cl-BQ	2-chloro-p-benzoquinone
Cl-HQ	Chlorohydroquinone
HQ	Hydroquinone
BQ	p-benzoquinone
2,5-DCBQ	2,5-dichloro-p-benzoquinone
2,5-DHBQ	2,5-dichloro-hydroquinone
2,4,5-TCP	2,4,5-trichlorophenol

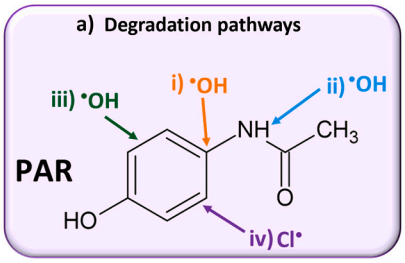

Na_2SO_4+NaCl	
Acronym	Full name
HQ	Hydroquinone
1-MCDD	1-chlorodibenzo-p-dioxin
Cl-HQ	Chlorohydroquinone
3,4-DCP	3,4-dichlorophenol
4-NC	4-nitrocatechol
1,3-BDO	1,3-benzenediol
3,4-DBA	3,4-dichlorobenzenamine

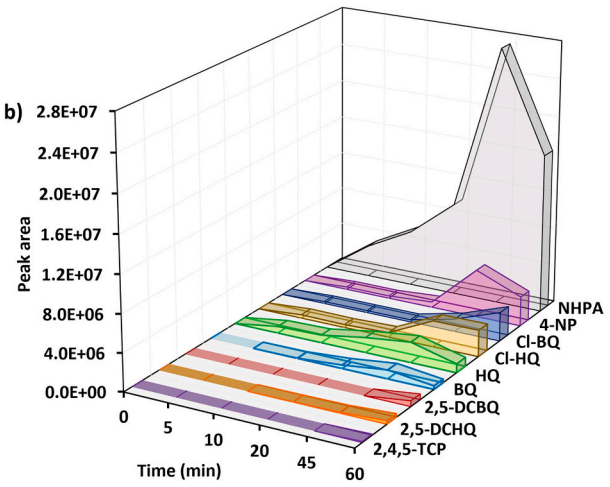

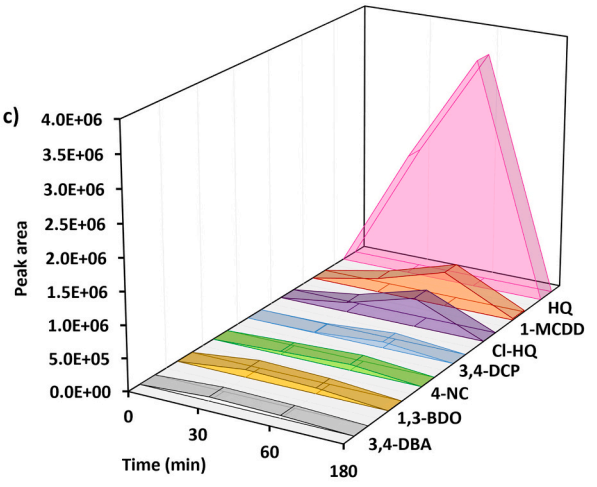

Fig. 4. Kinetics of the by-products identified during PAR, a) main pathways, b) electrolyte: NaCl and c) electrolyte: Na_2SO_4 + NaCl.

nearly complete degradation of the formed by-products can occur over the course of the experiment. HQ was the compound produced in the highest concentration, with a maximum at 60 min ($3.6 \cdot 10^6$). 1-MCDD is the compound that follows in terms of concentration (peak area at 60 min, $5.4 \cdot 10^5$). The rest of the compounds, Cl-HQ, 3,4-DCP, 4-NC, 1,3-DBO and 3,4-DBA are formed in a lower amount, with a peak area $<5 \cdot 10^5$, i.e., a concentration 10 times less than the concentration of HQ.

Lastly, in the case of sertraline, the available literature is scarce, just like the by-products analysis during electrochemical oxidation, being the photochemical processes the ones that have been more widely reported (Calza et al., 2021; Jiménez-Holgado et al., 2021). This research delves further into the analysis of the by-products generated from STR in two different electrolytic media during an ELOX process. It reveals the presence of various compounds that have not been previously detected, to the extent of the authors' knowledge. The main degradation/transformation pathway followed by STR in this work, and shown in Fig. 5a is i) the ring detachment, which takes place through •OH attack generating, on the one hand, compounds like 3,4-dichlorophenol (3,4-DCP) (Fig. 5b and c), or similar chlorophenolic compounds, as 3,4-DCS (Fig. 5b and c) and 3,4-DBA (Fig. 5c), and on the other hand, the rest of the STR molecule, such as MNA (Fig. 5b), or other naphthalene-like structures such as NAP (Fig. 5b) (Calza et al., 2021; Jiménez-Holgado et al., 2021). In chloride presence, also it could be supposed the formation of other chlorophenols, detected in this work, from the chlorination of 3,4-DCP, such as 2,4,5-TCP (Fig. 5b and c), 2,3,4-TCP (Fig. 5c), or 2,3,4,6-TeCP (Fig. 5b and c).

The kinetics of each one of the intermediates generated during STR degradation have been represented in Fig. 5b (NaCl medium) and in Fig. 5c (Na_2SO_4 + NaCl medium). As it can be appreciated in Fig. 5b, the generated by-products increase until a maximum at different times, ending with values close to zero, except for NAP, which culminations with a peak area of $1.1 \cdot 10^5$, at the final time, being one of the formed in the highest amount. This can also be attributed to the rapid degradation achieved with NaCl for STR (15 min), (as can be evidenced by the kinetic constants in Table S13). As a result of this, the formation of by-products occurs also very fast, as does their degradation. NAP can be originated from a larger fragment of STR (MNA, see Fig. 5b and structure in Table S6); which corresponds to the upper part of the STR molecule, generated from pathway (i) (Fig. 5a). Because it is a structure similar to PAHs, and as it has been described in the case of DEX, its degradation requires longer operation times. Then, 3,4-DCP and 3,4-DCS are the second and third compounds formed in higher concentration (in terms of peak area), achieving their top points at 8 min (peak areas between $1.8 \cdot 10^5$ and $2.4 \cdot 10^5$) (Fig. 5b). Furthermore, another chlorophenol is formed, 2,4,5-TCP, probably generated due to the chlorination of 3,4-DCP, since it started to appear at 5 min (with 3,4-DCP appearing at 2 min), reaching its greatest point at 8 min ($9.3 \cdot 10^4$). Then, MNA is the following compound, which corresponds to the upper part of the STR molecule (when the C—C middle bond breaks, Fig. 5a, (i)) (highest peak area at 12 min, $5.5 \cdot 10^4$). Finally, 2,3,4,6-TeCP is formed in lower concentration comparing it with the rest of the molecules, but constantly growing until the final experimental time (peak area of $3.1 \cdot 10^4$). Lastly, for the Na_2SO_4 + NaCl medium, it can be appreciated in Fig. 5c that all the compounds increase their peak area until achieve a maximum, and end with negligible values, except for the 3,4-DCP. 3,4-DCP is the compound with the highest concentration, with its peak at 80 min ($5.6 \cdot 10^6$), then it decays a bit (at 100 min) and grows again at the final experimental time (120 min) with a final value of $3.6 \cdot 10^6$. This chlorophenol directly arises from STR cleavage through the C—C bond between both parts of the molecule (generated from pathway (i), Fig. 5a). Its conversion/breakdown into other products is hindered, possibly due to molecule stability, accounting for its elevated concentration at the end of the experiment. The remaining by-products were formed in smaller quantities and degrade by the experiment's end due to

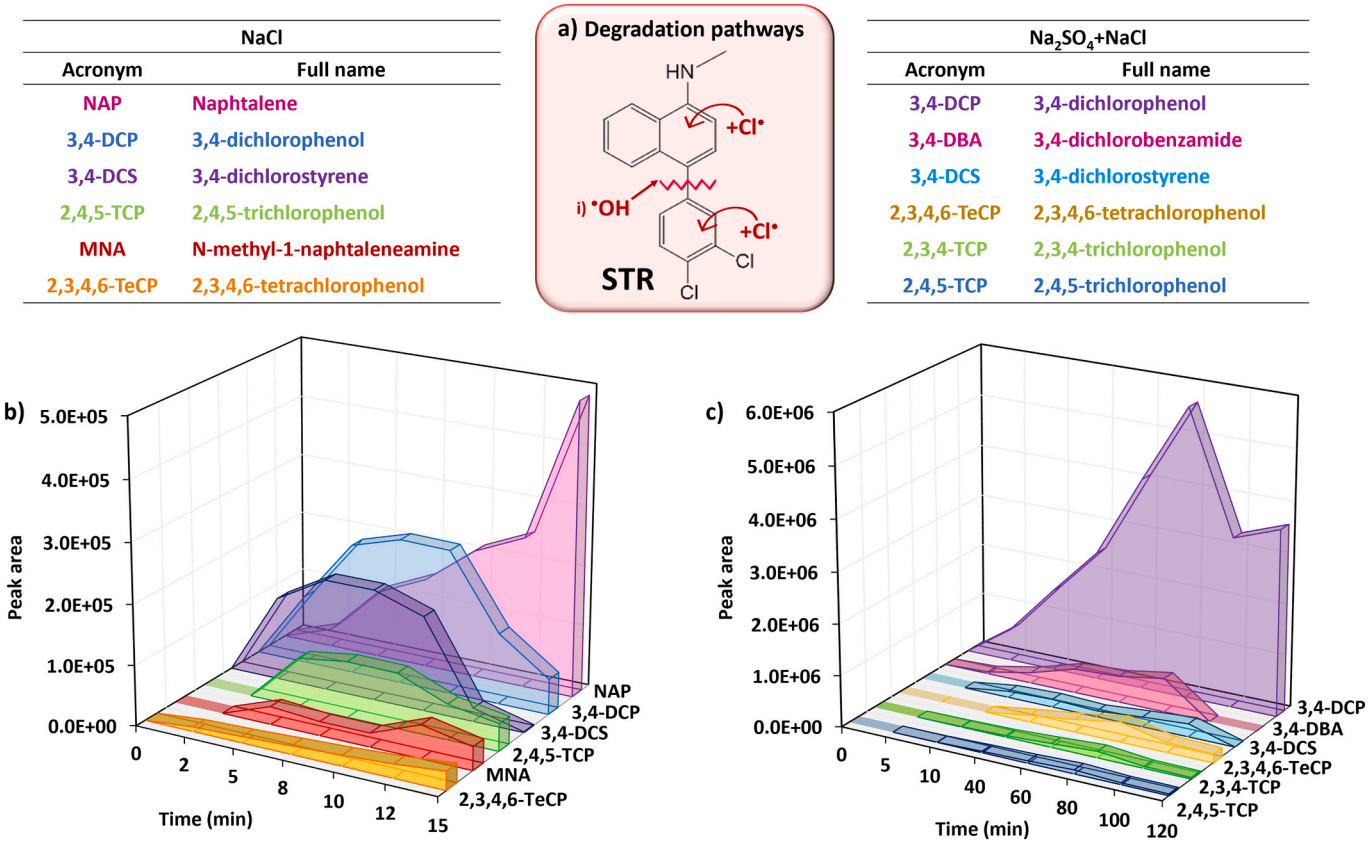

Fig. 5. Kinetics of the by-products identified during STR degradation, a) main pathways, b) electrolyte: NaCl and c) electrolyte: Na_2SO_4 + NaCl.

its duration and limited presence, as it is described hereunder. 3,4-DBA and 3,4-DCS and appears in the same order of magnitude ($\approx 10^5$). The rest of the compounds, 2,3,4,6-TeCP, 2,4,5-TCP and 2,3,4-TCP, possess lower peak area values, all of them under $4 \cdot 10^5$, being almost completely degraded at final time.

3.3. PCDD/Fs and toxicity (TEQ) analysis

As is well-known from the previous literature (Fernández-Castro et al., 2016; Schröder et al., 2021; Solá-Gutiérrez et al., 2019; Vallejo et al., 2013), and it has been shown in this work, when advanced oxidation processes are applied to treat drugs, even though the degradation of the parent compounds is usually complete (in general terms), depending on the compounds to degrade or the operating conditions, determined intermediate compounds can be generated during the oxidation process. The appearance of several chlorophenols in the electrochemical oxidation of the four pharmaceuticals, results in the formation of low-chlorinated dioxins and furans, by the condensation of two chlorophenols. Research by Sidhu and Edwards (2002) demonstrated that two 2-chlorophenoxy radicals (2-CPR) combine to preferentially form furans instead of dioxins (Fernández-Castro et al., 2016; Sidhu and Edwards, 2002). These radicals are produced from 2-chlorophenol (2-CP) precursors, which are radical active species that possess enol and keto forms with the unpaired electron on the phenolic oxygen. Since keto forms are more stable than enol forms, a higher formation of DCDF is expected (Fernández-Castro et al., 2016; Schröder et al., 2023). Finally, the radicals and oxidant species attack low-chlorinated PCDD/Fs, increasing the chlorination degree and resulting in higher chlorination degree 2,3,7,8-PCDD/Fs. PCDD/Fs can be even more hazardous than the parent compounds, which could lead to an increase in the final toxicity of the degraded sample.

In order to check this point, the electrochemical oxidation of aqueous solutions containing 10 mg L^{-1} of each drugs, DEX, AMX, PAR and STR, was carried out in a previous work, where the group of homologs of dioxins and furans was analysed (Schröder et al., 2023). Here, the research continues with the study of the congeners and their associated toxicity.

3.3.1. PCDD/Fs congeners analysis

In a first stage, regarding to the assessment of PCDD/Fs, the analysis of the 2,3,7,8-congeners was carried out. In Table 1 are gathered the 2,3,7,8-congeners concentrations, classified into 2,3,7,8-PCDDs and 2,3,7,8-PCDFs, with the correspondent percentages of its contribution to the total amount of congeners for each study case. Additionally, the congener profiles, for each pharmaceutical compound, are shown in Fig. 6 for the NaCl and Na_2SO_4 + NaCl electrolyte mediums. These congeners concentrations are represented in bar graphs, specifically, Fig. 6a, it is represented the congener profile for DEX, and consecutively, Fig. 6b, c and d represents the congener profiles for AMX, PAR and STR, respectively. It is necessary to remark the scale of the congener charts (Fig. 6), because it is decisive in the analysis and the further toxicity calculation, especially for the 2,3,7,8-TCDD case. This dioxin achieves the highest toxicity value (I-TEF = 1).

Table 1
Total amount (and percentage) of 2,3,7,8-PCDD/Fs congeners produced during the DEX, AMX, PAR and STR degradation, using NaCl and Na_2SO_4 + NaCl as electrolytes.

Drug	2,3,7,8-PCDDs pg L^{-1} (%)	2,3,7,8-PCDFs pg L^{-1} (%)	TOTAL 2,3,7,8-congeners pg L^{-1} (%)
	Electrolyte: 56 mM NaCl		
DEX	80.2 (83.5 %)	15.9 (16.5 %)	96.1 (100 %)
AMX	7.3 (2.9 %)	242.0 (97.1 %)	249.3 (100 %)
PAR	30.4 (44.2 %)	38.3 (55.8 %)	68.7 (100 %)
STR	60.4 (86.8 %)	9.2 (13.2 %)	69.6 (100 %)
	Electrolyte: 21 mM Na_2SO_4 + 2.8 mM NaCl		
DEX	46.8 (89.0 %)	5.8 (11.0 %)	52.6 (100 %)
AMX	4.6 (3.5 %)	126.2 (96.5 %)	130.8 (100 %)
PAR	20.9 (57.9 %)	15.2 (42.1 %)	36.1 (100 %)
STR	27.9 (67.1 %)	13.7 (32.9 %)	41.7 (100 %)

As depicted in Table 1, the total amount of 2,3,7,8-PCDD/Fs congeners is the highest in all cases when NaCl was employed as electrolyte, being in the range between 68.7 pg L^{-1} for the PAR up to 249.3 pg L^{-1} for the AMX. For the NaCl case, the dioxins congeners (2,3,7,8-PCDDs) were higher for DEX and STR, with values of 80.2 and 60.4 pg L^{-1}, accounting for 83.5 and 86.8 % of the total 2,3,7,8-congeners, respectively. Contrarily, for AMX and PAR, the furans congeners (2,3,7,8-PCDFs) were the predominating group, with values of 242.0 and 38.3 pg L^{-1}, i.e., the 97.1 and 55.8 % of the total 2,3,7,8-congeners, respectively. In the same way, as it is shown in Table 1, in the Na_2SO_4 + NaCl case, the highest total amount of 2,3,7,8-PCDD/Fs and 2,3,7,8-PCDFs were for AMX, reaching values of 130.8 pg L^{-1} and 126.2 pg L^{-1} (96.5 % of the total congeners for this case), respectively. The lowest amount of total PCDD/Fs congeners corresponded to PAR, 36.1 pg L^{-1}. The dioxin congeners were higher for DEX and STR, with values of 46.8 and 27.09 pg L^{-1}, accounting for 89.0 and 67.1 % of the total 2,3,7,8-congeners, respectively. Particularly, in the PAR oxidation, dioxins and furans congeners were formed approximately in the same amount, independently of the electrolyte used, so, for the NaCl case, 30.4 pg L^{-1} of PCDDs and 38.3 pg L^{-1} PCDFs were obtained (being the 44.2 % and 57.9 % of the total congeners amount) and for the Na_2SO_4 + NaCl case, 20.9 pg L^{-1} and 15.2 pg L^{-1} PCDDs and PCDFs, respectively (Table 1), which represents the 57.9 % and 42.1 % of the total congeners detected in the PAR oxidation.

The most toxic dioxin, 2,3,7,8-TCDD was found in very low concentrations, but it is important to not underestimate this concentration, because it has the highest toxicity factor (I-TEF = 1). In this work, the concentrations were, for NaCl electrolyte, 2.0, 0.8 and 0.6 pg L^{-1} for DEX, PAR and STR (Fig. 6a, c and d), respectively; and for Na_2SO_4 + NaCl electrolyte, 0.2, 0.4 and 0.4 pg L^{-1} for DEX, PAR and STR, respectively (Fig. 6a, c and d). It was not detected in AMX electro-oxidated samples (Fig. 6b). Specifically, in the DEX degradation, it should be remarked that the 1,2,3,7,8-PeCDD congener, which is the highest formed congener for both electrolytes, reached very similar values: 49.7 and 43.7 pg L^{-1} (51.7 and 83.1 % of the total DEX congeners amount) for NaCl and Na_2SO_4 + NaCl, respectively (Fig. 6a). Regarding AMX, the 1,2,3,4,6,7,8-HpCDF is the congener with higher concentration, 234.6 pg L^{-1} (NaCl) and 117.6 pg L^{-1} (Na_2SO_4 + NaCl), which represents 94.1 % and 89.9 %, respectively of the total 2,3,7,8-PCDD/Fs, so therefore, the concentration of the rest congeners, it is considered practically negligible (Fig. 6b). In the PAR oxidation, 1,2,3,4,6,7,8-HpCDF is the congener that reached the highest concentration, also for both electrolytes, 29.7 pg L^{-1}, i.e., 43.2 % of the total 2,3,7,8-PCDD/Fs amount in medium NaCl and 14.4 pg L^{-1}, i.e., 39.8 % of the total 2,3,7,8-PCDD/Fs amount in medium Na_2SO_4 + NaCl (Fig. 6c). Lastly, for the STR case, there are two congeners with higher concentrations in both electrolytes medium, these congeners are the 1,2,3,7,8-PeCDD and the 1,2,3,6,7,8-HxCDD, being those concentrations 29.9 and 25.0 pg L^{-1} for NaCl, respectively (representing 42.9 % and 35.9 % of the total STR-congeners) and 10.0 and 16.8 for Na_2SO_4 + NaCl, respectively (23.9 and 40,3 % of the total congeners) (Fig. 6d).

3.3.2. Toxicity analysis in terms of TEQ

The congeners analysis allows the estimation of the toxicity of a sample in terms of equivalent toxicity (TEQ). The value of TEQ is calculated using Eq. (1), as the sum of the product of each 2,3,7,8-PCDD/Fs congener concentration and the corresponding I-TEF (International Toxic Equivalent Factors) (I-TEF values represented in Table S14):

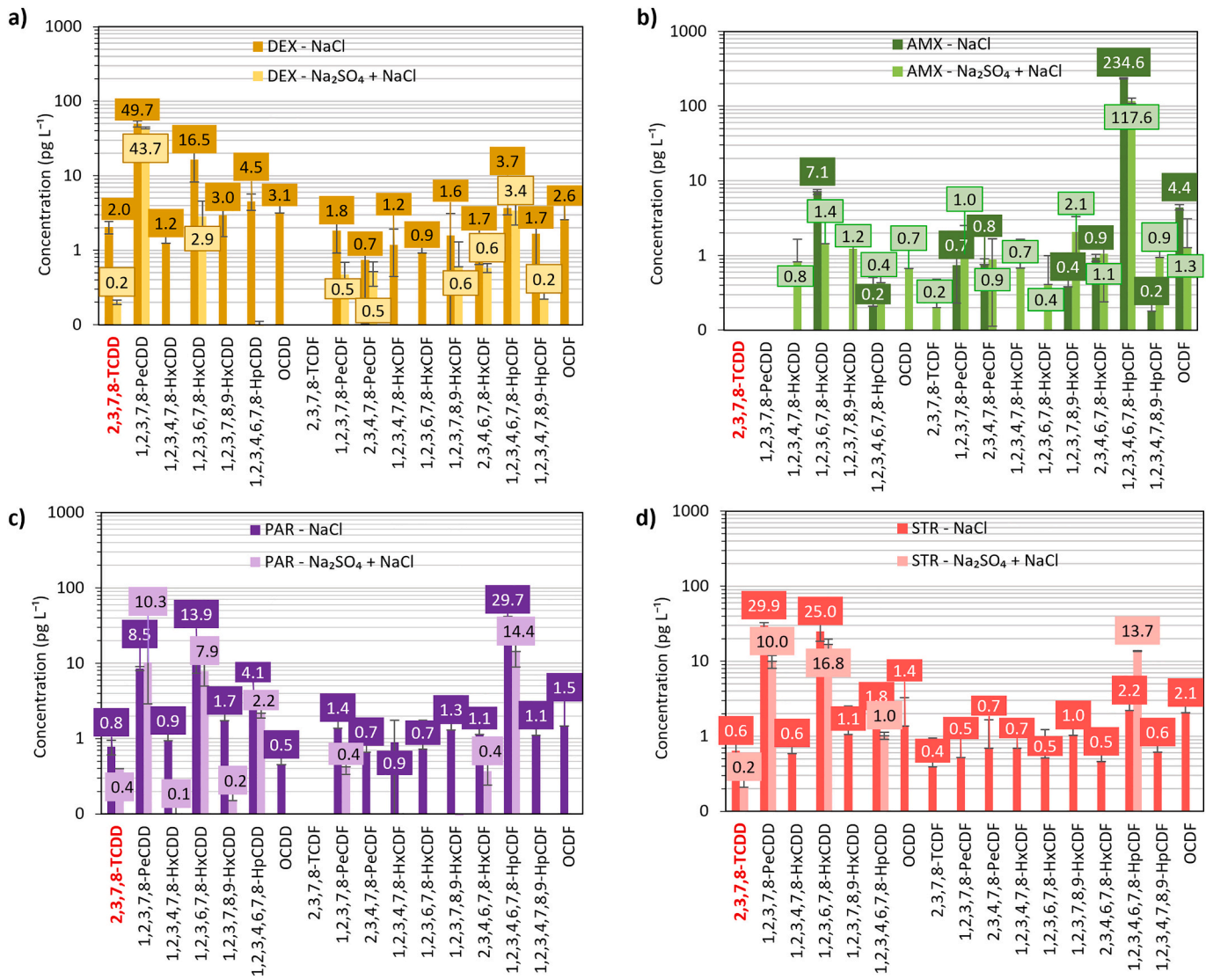

Fig. 6. 2,3,7,8-PCDD/Fs congeners profile of the ELOX experiments of a) DEX, b) AMX, c) PAR and d) STR, for the electrolytic media, 56 mM NaCl and 21 mM Na_2SO_4 + 2.8 mM NaCl.

$$TEQ = \sum_i (PCDD_i \cdot ITEF_i) + \sum_j (PCDF_j \cdot ITEF_j) \quad (1)$$

where i and j correspond to the respective number of PCDD and PCDF congeners, respectively.

In Fig. 7 is depicted the toxicity associated with each sample, for each drug and electrolyte medium, calculated through the congeners measured at the final time of each electrochemical experiment, which is, when the pharmaceutical compound has been completely degraded.

Fig. 7 shows that the greater toxicity value belongs to DEX using both electrolytes, 30.1 pg L^{-1} for NaCl and 22.8 pg L^{-1} for Na_2SO_4 + NaCl. The main contribution to these values is due to the higher amounts of the 1,2,3,7,8-PeCDD congener (purple colour), 49.7 (NaCl, Fig. 6a) and 43.7 pg L^{-1} (Na_2SO_4 + NaCl, Fig. 6a), and to the value of toxicity factor, I-TEF = 0.5, the second highest between I-TEF value (Table S14). 2,3,7,8-TCDD (red colour), the most toxic congener (I-TEF = 1), was present in concentrations of 2.0 (NaCl, Fig. 6a) and 0.4 pg L^{-1} (Na_2SO_4 + NaCl, Fig. 6a), contributing minimally to the total toxicity. STR is the next compound in toxicity terms despite, its low total congeners' concentrations, 69.6 and 41.7 pg L^{-1} for NaCl (Fig. 6d) and Na_2SO_4 + NaCl (Fig. 6d), respectively (Table 1). Again, this situation is associated with the combination of the concentration and I-TEF of the formed congeners.

For the NaCl case, TEQ was 19.0 pg L^{-1}, being the congeners, 1,2,3,7,8-PeCDD (purple colour) with 30 pg L^{-1} (Fig. 6d) and I-TEF = 0.5 and 1,2,3,6,7,8-HxCDD (pink colour) with 25.0 pg L^{-1} (Fig. 6d) and I-TEF = 0.1, those which contribute the most to the total toxicity. A similar reading can be made for the case of electrolytic medium Na_2SO_4 + NaCl, the (TEQ = 7 pg L^{-1}). 2,3,7,8-TCDD (red colour), was present in concentrations of 0.64 (NaCl, Fig. 6d) and 0.40 pg L^{-1} (Na_2SO_4 + NaCl, Fig. 6d). Once more, the contribution of the most toxic congener to TEQ was minimal. Subsequently, degraded PAR solutions appear in third place in TEQ terms, reaching values up to 7.9 pg L^{-1} (NaCl, Fig. 6c) and 6.6 pg L^{-1} (Na_2SO_4 + NaCl, Fig. 6c). In this case, the highest concentration congener formed for both electrolytic media was 1,2,3,4,6,7,8-HpCDF (light green colour), with 29.7 pg L^{-1} (NaCl, Fig. 6c) and 14.4 pg L^{-1} (Na_2SO_4 + NaCl, Fig. 6c), however, its contribution to the total toxicity was minimal, due to that I-TEF is 0.01. As in the previous cases, the congeners 1,2,3,7,8-PeCDD congener (purple colour) and 1,2,3,6,7,8-HxCDD (pink colour) are the ones that contribute the most to the total toxicity. In these samples, 2,3,7,8-TCDD (red colour), was found with values of 0.8 (NaCl, Fig. 6c) and 0.4 pg L^{-1} (Na_2SO_4 + NaCl, Fig. 6c). Opposite, and surprisingly, in the last case, the AMX gives the lowest toxicity values, even though it possesses the highest values of the total concentration of the 2,3,7,8-congeners, 249.3 (NaCl, Fig. 6b) and

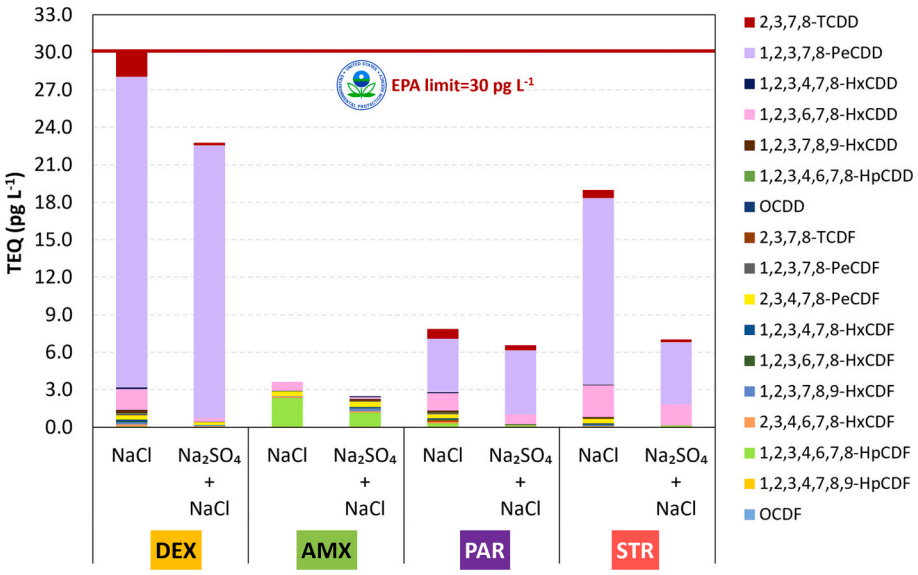

Fig. 7. Final toxicity, expressed in terms of TEQ, for the four degraded drugs: DEX, AMX, PAR and STR (NaCl and Na_2SO_4 + NaCl).

130.8 pg L^{-1} (Na_2SO_4 + NaCl, Fig. 6b) (Table 1). Despite that the congener 1,2,3,4,6,7,8-HpCDF (light green colour) presented the highest concentration, 234.6 pg L^{-1} when using NaCl (Fig. 6b), it did not provide elevated toxicity to the reaction medium, because its low I-TEF value, 0.01. These results contribute to the total toxicity of AMX in 3.6 pg L^{-1} of TEQ (NaCl). The same conclusion can be obtained for Na_2SO_4 electrolyte. It is worth to recall that the limit established by the US EPA is 30 pg L^{-1} (US EPA, 2013), so the value determined here is above the allowed threshold for DEX in NaCl medium. This findings are of great importance as, here, it is specifically calculated for individual and synthetic drug samples. Real samples, on the other hand, can contain hundreds of additional compounds, which may result in significantly higher levels of toxicity. Therefore, this study not only establishes a robust methodology but also presents decisive findings regarding the assessment of wastewater quality after treatment in WWTPs, and after the application of an AOPs, which should be meticulously selected, with particular emphasis on the type of matrix and in the operating variables.

4. Conclusions

Water pollution from pharmaceuticals has emerged as a significant concern in recent decades. The presence of drugs in water sources worldwide necessitates efforts to address this issue, with a particular focus on improving wastewater treatment methods. In this study, electrochemical oxidation was employed to remediate highly concentrated solutions containing drugs: dexamethasone, amoxicillin, paracetamol and sertraline. A thorough analysis of the intermediate by-products generated during the ELOX process was conducted for the four drugs investigated in this research. The presence of several chlorophenols, hydroquinones and benzoquinones, alongside various derivatives of the parent compounds, was observed. Furthermore, an evaluation of the PCDD/F congeners was undertaken to assess the final toxicity of the samples. Notably, the total concentration of congeners was found to be higher when NaCl was used as the electrolytic medium, reaching levels as high as 249.3 pg L^{-1}. Although the most toxic dioxin, 2,3,7,8-TCDD, was detected in low concentrations (up to 2.04 pg L^{-1}). The overall toxicity levels reached values as high as 30.1 pg L^{-1} of toxic equivalent (TEQ) when DEX was treated with NaCl. This finding was attributed to the elevated presence of other congeners with relatively lower toxicity (1,2,3,7,8-PeCDD, I-TEF = 0.5). These results emphasize the significance of considering the impact of congeners with lesser toxicity, as they can significantly contribute to the overall toxicity of a sample. The formation of by-products poses a critical challenge in the application of advanced oxidation processes (AOPs) to solutions containing organic compounds, particularly those that may act as potential precursors of PCDD/Fs. Thus, the careful selection of operating conditions, such as the choice of electrolytic media, becomes essential to minimize the potential production of PCDD/Fs and their precursor compounds.

CRediT authorship contribution statement

Sophie Schröder: Conceptualization, Formal analysis, Investigation, Methodology, Writing – original draft, Writing – review & editing.
Inmaculada Ortiz: Formal analysis, Review.
Ma.-Fresnedo San-Román: Conceptualization, Formal analysis, Funding acquisition, Investigation, Resources, Methodology, Project administration, Supervision, Writing – review & editing.

Declaration of competing interest

The authors declare that they have no known competing financial interests or personal relationships that could have appeared to influence the work reported in this paper.

Data availability

The data that has been used is confidential.

Acknowledgements

This research was developed in the framework of the project PID2020-115409RB-I00 (MCIN/AEI) financed by the Spanish Ministry of Science and Innovation. Sophie Schröder is also grateful for the FPI predoctoral contract, PRE2018-083526.

Appendix A. Supplementary data

Supplementary data to this article can be found online at https://doi.org/10.1016/j.scitotenv.2023.167660.

References

Abajo, Z., Jimenez, A., Domingo-Echaburu, S., Valcárcel, Y., Segura, Y., Orive, G., Lertxundi, U., 2023. Analyzing the potential environmental impact of NIOSH list of

hazardous drugs (group 2). Sci. Total Environ. 873 https://doi.org/10.1016/j.scitotenv.2023.162280.
Akhter, S., Bhat, M.A., Ahmed, S., Siddiqi, W.A., Ahmad, S., Shrimal, H., 2023. Profiling of antibiotic residues in surface water of River Yamuna stretch passing through Delhi, India. Water (Switzerland) 15. https://doi.org/10.3390/w15030527.
Alharbi, O.A., Jarvis, E., Galani, A., Thomaidis, N.S., Nika, M.C., Chapman, D.V., 2023. Assessment of selected pharmaceuticals in Riyadh wastewater treatment plants, Saudi Arabia: mass loadings, seasonal variations, removal efficiency and environmental risk. Sci. Total Environ. 882, 163284 https://doi.org/10.1016/j.scitotenv.2023.163284.
Al-sareji, O.J., Meiczinger, M., Somogyi, V., Al-Juboori, R.A., Grmasha, R.A., Stenger-Kovács, C., Jakab, M., Hashim, K.S., 2023. Removal of emerging pollutants from water using enzyme-immobilized activated carbon from coconut shell. J. Environ. Chem. Eng. 11 https://doi.org/10.1016/j.jece.2023.109803.
Angeles-de Paz, G., León-Morcillo, R., Guzmán, S., Robledo-Mahón, T., Pozo, C., Calvo, C., Aranda, E., 2023. Pharmaceutical active compounds in sewage sludge: degradation improvement and conversion into an organic amendment by bioaugmentation-composting processes. Waste Manag. 168, 167–178. https://doi.org/10.1016/j.wasman.2023.05.055.
Arun, K.B., Madhavan, A., Tarafdar, A., Sirohi, R., Anoopkumar, A.N., Kuriakose, L.L., Awasthi, M.K., Binod, P., Varjani, S., Sindhu, R., 2023. Filamentous fungi for pharmaceutical compounds degradation in the environment: a sustainable approach. Environ. Technol. Innov. 31, 103182 https://doi.org/10.1016/j.eti.2023.103182.
Äystö, L., Vieno, N., Fjäder, P., Mehtonen, J., Nystén, T., 2023. Hospitals and households as primary emission sources for risk-posing pharmaceuticals in municipal wastewater. Ecotoxicol. Environ. Saf. 262 https://doi.org/10.1016/j.ecoenv.2023.115149.
Babu, B.R., Venkatesan, P., Kanimozhi, R., Basha, C.A., 2009. Removal of pharmaceuticals from wastewater by electrochemical oxidation using cylindrical flow reactor and optimization of treatment conditions. J. Environ. Sci. Health Part A Toxic/Hazard. Subst. Environ. Eng. 44, 985–994. https://doi.org/10.1080/10934520902996880.
Binh, V.N., Dang, N., Anh, N.T.K., Ky, L.X., Thai, P.K., 2018. Antibiotics in the aquatic environment of Vietnam: sources, concentrations, risk and control strategy. Chemosphere 197, 438–450. https://doi.org/10.1016/j.chemosphere.2018.01.061.
Calza, P., Pelizzetti, E., Brussino, M., Baiocchi, C., 2001. Ion trap tandem mass spectrometry study of dexamethasone transformation products on light activated TiO2 surface. J. Am. Soc. Mass Spectrom. 12, 1286–1295. https://doi.org/10.1016/S1044-0305(01)00319-1.
Calza, P., Jiménez-Holgado, C., Coha, M., Chrimatopoulos, C., Dal Bello, F., Medana, C., Sakkas, V., 2021. Study of the photoinduced transformations of sertraline in aqueous media. Sci. Total Environ. 756, 143805 https://doi.org/10.1016/j.scitotenv.2020.143805.
Cantalupi, A., Maraschi, F., Pretali, L., Albini, A., Nicolis, S., Ferri, E.N., Profumo, A., Speltini, A., Sturini, M., 2020. Glucocorticoids in freshwaters: degradation by solar light and environmental toxicity of the photoproducts. Int. J. Environ. Res. Public Health 17, 1–15. https://doi.org/10.3390/ijerph17238717.
De Luna, M.D.G., Veciana, M.L., Su, C.C., Lu, M.C., 2012. Acetaminophen degradation by electro-Fenton and photoelectro-Fenton using a double cathode electrochemical cell. J. Hazard. Mater. 217–218, 200–207. https://doi.org/10.1016/j.jhazmat.2012.03.018.
Diaz-Camal, N., Cardoso-Vera, J.D., Islas-Flores, H., Gómez-Oliván, L.M., Mejía-García, A., 2022. Consumption and ocurrence of antidepressants (SSRIs) in pre- and post-COVID-19 pandemic, their environmental impact and innovative removal methods: a review. Sci. Total Environ. 829 https://doi.org/10.1016/j.scitotenv.2022.154656.
Farhat, A., Keller, J., Tait, S., Radjenovic, J., 2015. Removal of persistent organic contaminants by electrochemically activated sulfate. Environ. Sci. Technol. 49, 14326–14333. https://doi.org/10.1021/acs.est.5b02705.
Fernández-Castro, P., San Román, M.F., Ortiz, I., 2016. Theoretical and experimental formation of low chlorinated dibenzo-p-dioxins and dibenzofurans in the Fenton oxidation of chlorophenol solutions. Chemosphere 161, 136–144. https://doi.org/10.1016/j.chemosphere.2016.07.011.Ç.
Ferreira, M., Kuzniarska-Biernacka, I., Fonseca, A.M., Neves, I.C., Soares, O.S.G.P., Pereira, M.F.R., Figueiredo, J.L., Parpot, P., 2020. Electrochemical oxidation of amoxicillin on carbon nanotubes and carbon nanotube supported metal modified electrodes. Catal. Today 357, 322–331. https://doi.org/10.1016/j.cattod.2019.06.039.
Frontistis, Z., Antonopoulou, M., Venieri, D., Konstantinou, I., Mantzavinos, D., 2017. Boron-doped diamond oxidation of amoxicillin pharmaceutical formulation: statistical evaluation of operating parameters, reaction pathways and antibacterial activity. J. Environ. Manag. 195, 100–109. https://doi.org/10.1016/j.jenvman.2016.04.035.
Ganiyu, S.O., Oturan, N., Raffy, S., Cretin, M., Esmilaire, R., van Hullebusch, E., Esposito, G., Oturan, M.A., 2016. Sub-stoichiometric titanium oxide (Ti4O7) as a suitable ceramic anode for electrooxidation of organic pollutants: a case study of kinetics, mineralization and toxicity assessment of amoxicillin. Water Res. 106, 171–182. https://doi.org/10.1016/j.watres.2016.09.056.
Ganiyu, S.O., Oturan, N., Raffy, S., Cretin, M., Causserand, C., Oturan, M.A., 2019. Efficiency of plasma elaborated sub-stoichiometric titanium oxide (Ti4O7) ceramic electrode for advanced electrochemical degradation of paracetamol in different electrolyte media. Sep. Purif. Technol. 208, 142–152. https://doi.org/10.1016/j.seppur.2018.03.076.
Gary Mallard, W., Reed, J., 1997. Automated Mass Spectral Deconvolution & Identification System (AMDIS) - User Guide, National Institute of Standards and Technology (NIST) Standard Reference Data Program. U.S. Department of Commerce Technology Administration.
Ghanbari, F., Hassani, A., Wacławek, S., Wang, Z., Matyszczak, G., Lin, K.Y.A., Dolatabadi, M., 2021. Insights into paracetamol degradation in aqueous solutions by ultrasound-assisted heterogeneous electro-Fenton process: key operating parameters, mineralization and toxicity assessment. Sep. Purif. Technol. 266 https://doi.org/10.1016/j.seppur.2021.118533.
Ghenaatgar, A., Tehrani, M.A., Khadir, A., 2019. Photocatalytic degradation and mineralization of dexamethasone using WO3 and ZrO2 nanoparticles: optimization of operational parameters and kinetic studies. J. Water Process Eng. 32, 100969 https://doi.org/10.1016/j.jwpe.2019.100969.
Gornik, T., Kovacic, A., Heath, E., Hollender, J., Kosjek, T., 2020. Biotransformation study of antidepressant sertraline and its removal during biological wastewater treatment. Water Res. 181, 115864 https://doi.org/10.1016/j.watres.2020.115864.
Grilla, E., Taheri, M.E., Miserli, K., Venieri, D., Konstantinou, I., Mantzavinos, D., 2021. Degradation of dexamethasone in water using BDD anodic oxidation and persulfate: reaction kinetics and pathways. J. Chem. Technol. Biotechnol. 96, 2451–2460. https://doi.org/10.1002/jctb.6833.
Guo, Z., Guo, A., Guo, Q., Rui, M., Zhao, Y., Zhang, H., Zhu, S., 2017. Decomposition of dexamethasone by gamma irradiation: kinetics, degradation mechanisms and impact on algae growth. Chem. Eng. J. 307, 722–728. https://doi.org/10.1016/j.cej.2016.08.138.
Hawash, H.B., Moneer, A.A., Galhoum, A.A., Elgarahy, A.M., Mohamed, W.A.A., Samy, M., El-Seedi, H.R., Gaballah, M.S., Mubarak, M.F., Attia, N.F., 2023. Occurrence and spatial distribution of pharmaceuticals and personal care products (PPCPs) in the aquatic environment, their characteristics, and adopted legislations. J. Water Process Eng. 52, 103490 https://doi.org/10.1016/j.jwpe.2023.103490.
Jiménez-Holgado, C., Sakkas, V., Richard, C., 2021. Phototransformation of three psychoactive drugs in presence of sedimental water extractable organic matter. Molecules 26, 1–17. https://doi.org/10.3390/molecules26092466.
Korkmaz, N.E., Caglar, N.B., Aksu, A., Unsal, T., Balcıoglu, E.B., Cavus Arslan, H., Demirel, N., 2023. Occurrence, bioconcentration, and human health risks of pharmaceuticals in biota in the Sea of Marmara, Türkiye. Chemosphere 325, 138296. https://doi.org/10.1016/j.chemosphere.2023.138296.
Kumar, M., Silori, R., Mazumder, P., Tauseef, S.M., 2023. Screening of pharmaceutical and personal care products (PPCPs) along wastewater treatment system equipped with root zone treatment: a potential model for domestic waste leachate management. J. Environ. Manag. 335, 117494 https://doi.org/10.1016/j.jenvman.2023.117494.
Le, T.X.H., Van Nguyen, T., Amadou Yacouba, Z., Zoungrana, L., Avril, F., Nguyen, D.L., Petit, E., Mendret, J., Bonniol, V., Bechelany, M., Lacour, S., Lesage, G., Cretin, M., 2017. Correlation between degradation pathway and toxicity of acetaminophen and its by-products by using the electro-Fenton process in aqueous media. Chemosphere 172, 1–9. https://doi.org/10.1016/j.chemosphere.2016.12.060.
Lei, Y., Cheng, S., Luo, N., Yang, X., An, T., 2019. Rate constants and mechanisms of the reactions of Cl• and Cl2•− with trace organic contaminants. Environ. Sci. Technol. https://doi.org/10.1021/acs.est.9b02462.
Liu, Y.J., Hu, C.Y., Lo, S.L., 2019. Direct and indirect electrochemical oxidation of amine-containing pharmaceuticals using graphite electrodes. J. Hazard. Mater. 366, 592–605. https://doi.org/10.1016/j.jhazmat.2018.12.037.
Markic, M., Cvetnic, M., Ukic, S., Kusic, H., Bolanca, T., Bozic, A.L., 2018. Influence of process parameters on the effectiveness of photooxidative treatment of pharmaceuticals. J. Environ. Sci. Health Part A Toxic/Hazard. Subst. Environ. Eng. 53, 338–351. https://doi.org/10.1080/10934529.2017.1401394.
Moghaddam, A., Khayatan, D., Esmaeili Fard Barzegar, P., Ranjbar, R., Yazdanian, M., Tahmasebi, E., Alam, M., Abbasi, K., Esmaeili Gouvarchin Ghaleh, H., Tebyaniyan, H., 2023. Biodegradation of pharmaceutical compounds in industrial wastewater using biological treatment: a comprehensive overview. Int. J. Environ. Sci. Technol. https://doi.org/10.1007/s13762-023-04880-2 (Springer Berlin Heidelberg).
Morales-Paredes, C.A., Rodríguez-Díaz, J.M., Boluda-Botella, N., 2022. Pharmaceutical compounds used in the COVID-19 pandemic: a review of their presence in water and treatment techniques for their elimination. Sci. Total Environ. 814 https://doi.org/10.1016/j.scitotenv.2021.152691.
Musee, N., Kebaabetswe, L.P., Tichapondwa, S., Tubatsi, G., Mahaye, N., Learen, g, S.K., Nomngongo, P.N., 2021. Occurrence, fate, effects, and risks of dexamethasone: ecological implications post-covid-19. Int. J. Environ. Res. Public Health 18. https://doi.org/10.3390/ijerph182111291.
Olvera-Vargas, H., Rouch, J.C., Coetsier, C., Cretin, M., Causserand, C., 2018. Dynamic cross-flow electro-Fenton process coupled to anodic oxidation for wastewater treatment: application to the degradation of acetaminophen. Sep. Purif. Technol. 203, 143–151. https://doi.org/10.1016/j.seppur.2018.03.063.
Pariente, M.I., Segura, Y., Álvarez-Torrellas, S., Casas, J.A., de Pedro, Z.M., Diaz, E., García, J., López-Muñoz, M.J., Marugán, J., Mohedano, A.F., Molina, R., Munoz, M., Pablos, C., Perdigón-Melón, J.A., Petre, A.L., Rodríguez, J.J., Tobajas, M., Martínez, F., 2022. Critical review of technologies for the on-site treatment of hospital wastewater: from conventional to combined advanced processes. J. Environ. Manag. 320 https://doi.org/10.1016/j.jenvman.2022.115769.
Patel, M., Kumar, R., Kishor, K., Mlsna, T., Pittman, C.U., Mohan, D., 2019. Pharmaceuticals of emerging concern in aquatic systems: chemistry, occurrence, effects, and removal methods. Chem. Rev. 119, 3510–3673. https://doi.org/10.1021/acs.chemrev.8b00299.
Pazoki, M., Parsa, M., Farhadpour, R., 2016. Removal of the hormones dexamethasone (DXM) by Ag doped on TiO2 photocatalysis. J. Environ. Chem. Eng. 4, 4426–4434. https://doi.org/10.1016/j.jece.2016.09.034.

Periyasamy, S., Muthuchamy, M., 2018. Electrochemical oxidation of paracetamol in water by graphite anode: effect of pH, electrolyte concentration and current density. J. Environ. Chem. Eng. 6, 7358–7367. https://doi.org/10.1016/j.jece.2018.08.036.

Pretali, L., Albini, A., Cantalupi, A., Maraschi, F., Nicolis, S., Sturini, M., 2021. Tio2-photocatalyzed water depollution, a strong, yet selective depollution method: new evidence from the solar light induced degradation of glucocorticoids in freshwaters. Appl. Sci. 11 https://doi.org/10.3390/app11062486.

Quaresma, A.V., Rubio, K.T.S., Taylor, J.G., Sousa, B.A., Silva, S.Q., Werle, A.A., Afonso, R.J.C.F., 2021. Removal of dexamethasone by oxidative processes: structural characterization of degradation products and estimation of the toxicity. J. Environ. Chem. Eng. 9, 106884 https://doi.org/10.1016/j.jece.2021.106884.

Rabeea, S.A., Merchant, H.A., Khan, M.U., Kow, C.S., Hasan, S.S., 2021. Surging trends in prescriptions and costs of antidepressants in England amid COVID-19. J. Pharm. Sci. 29, 217–221. https://doi.org/10.1007/s40199-021-00390-z.

Rajasekhara, B., Nambia, I.M., Govindarajanb, S.K., 2021. Investigating the degradation of nC12 to nC23 alkanes and PAHs in petroleum- contaminated water by electrochemical advanced oxidation process using an inexpensive Ti/Sb-SnO_2/PbO_2 anode. Chem. Eng. J. 404, 125268 https://doi.org/10.1016/j.cej.2020.125268.

Rapp-Wright, H., Regan, F., White, B., Barron, L.P., 2023. A year-long study of the occurrence and risk of over 140 contaminants of emerging concern in wastewater influent, effluent and receiving waters in the Republic of Ireland. Sci. Total Environ. 860 https://doi.org/10.1016/j.scitotenv.2022.160379.

Rasolevandi, T., Naseri, S., Azarpira, H., Mahvi, A.H., 2019. Photo-degradation of dexamethasone phosphate using UV/Iodide process: kinetics, intermediates, and transformation pathways. J. Mol. Liq. 295, 111703 https://doi.org/10.1016/j.molliq.2019.111703.

Saha, P., Wang, J., Zhou, Y., Carlucci, L., Jeremiasse, A.W., Rijnaarts, H.H.M., Bruning, H., 2022. Effect of electrolyte composition on electrochemical oxidation: active sulfate formation, benzotriazole degradation, and chlorinated by-products distribution. Environ. Res. 211, 113057 https://doi.org/10.1016/j.envres.2022.113057.

Schröder, S., San-Román, M.F., Ortiz, I., 2020. Photocatalytic transformation of triclosan. Reaction products and kinetics. Catalysts 10, 1–15. https://doi.org/10.3390/catal10121468.

Schröder, S., San-Román, M.F., Ortiz, I., 2021. Dioxins and furans toxicity during the photocatalytic remediation of emerging pollutants. Triclosan as case study. Sci. Total Environ. 770, 144853 https://doi.org/10.1016/j.scitotenv.2020.144853.

Schröder, S., Ortiz, I., San-Román, M.-F., 2023. Formation of polychlorinated dibenzo-p-dioxins and furans (PCDD/Fs) in the electrochemical oxidation of polluted waters with pharmaceuticals used against COVID-19. J. Environ. Chem. Eng. 11, 109305 https://doi.org/10.1016/j.jece.2023.109305.

Siciliano, A., Guida, M., Libralato, G., Saviano, L., Luongo, G., Previtera, L., Di Fabio, G., Zarrelli, A., 2021. Amoxicillin in water: insights into relative reactivity, byproduct formation, and toxicological interactions during chlorination. Appl. Sci. 11, 1–12. https://doi.org/10.3390/app11031076.

Sidhu, S., Edwards, P., 2002. Role of phenoxy radicals in PCDD/F formation. Int. J. Chem. Kinet. 34, 531–541. https://doi.org/10.1002/kin.10083.

Solá-Gutiérrez, C., San Román, M.F., Ortiz, I., 2018. Fate and hazard of the electrochemical oxidation of triclosan. Evaluation of polychlorodibenzo-p-dioxins and polychlorodibenzofurans (PCDD/Fs) formation. Sci. Total Environ. 626, 126–133. https://doi.org/10.1016/j.scitotenv.2018.01.082.

Solá-Gutiérrez, C., Schröder, S., San Román, M.F., Ortiz, I., 2019. PCDD/Fs traceability during triclosan electrochemical oxidation. J. Hazard. Mater. 369, 584–592. https://doi.org/10.1016/j.jhazmat.2019.02.066.

Sulaiman, S., Khamis, M., Nir, S., Lelario, F., Scrano, L., Bufo, S.A., Karaman, R., 2014. Stability and removal of dexamethasone sodium phosphate from wastewater using modified clays. Environ. Technol. (United Kingdom) 35, 1945–1955. https://doi.org/10.1080/09593330.2014.888097.

Sun, R., Huang, W., Zhang, Q., Hong, J. ming, 2018. Facilely prepared N-doped graphene/Pt/TiO2 as an efficient anode for acetaminophen degradation. Catal. Lett. 148, 2418–2431. https://doi.org/10.1007/s10562-018-2466-5.

Tan, T.Y., Zeng, Z.T., Zeng, G.M., Gong, J.L., Xiao, R., Zhang, P., Song, B., Tang, W.W., Ren, X.Y., 2020. Electrochemically enhanced simultaneous degradation of sulfamethoxazole, ciprofloxacin and amoxicillin from aqueous solution by multi-walled carbon nanotube filter. Sep. Purif. Technol. 235, 116167 https://doi.org/10.1016/j.seppur.2019.116167.

US EPA, 1994. Method 1613B Tetra- Through Octa-chlorinated Dioxins and Furans by Isotope Dilution HRGC/HRMS. Environ. Prot.

US EPA, 1998. Method 8270D Semivolatile Organic Compounds By Gas Chromatography/Mass Spectrometry (GC/MS). EPA Method.

US EPA, 2007. Method 8041A Phenols by Gas Chromatography. EPA Method, pp. 1–30.

US EPA, 2013. National Primary Drinking Water Regulations. Drink. Water Contam, pp. 141–142.

Vallejo, M., San Román, M.F., Ortiz, I., 2013. Quantitative assessment of the formation of polychlorinated derivatives, PCDD/Fs, in the electrochemical oxidation of 2-chlorophenol as function of the electrolyte type. Environ. Sci. Technol. 47, 12400–12408. https://doi.org/10.1021/es403246g.

Vallejo, M., San Román, M.F., Ortiz, I., Irabien, A., 2014. The critical role of the operating conditions on the Fenton oxidation of 2-chlorophenol: assessment of PCDD/Fs formation. J. Hazard. Mater. 279, 579–585. https://doi.org/10.1016/j.jhazmat.2014.07.020.

Waterston, K., Wang, J.W., Bejan, D., Bunce, N.J., 2006. Electrochemical waste water treatment: electrooxidation of acetaminophen. J. Appl. Electrochem. 36, 227–232. https://doi.org/10.1007/s10800-005-9049-z.

WHO, UNICEF, 2020. Water, Sanitation, Hygiene and Waste Management for the COVID-19 Virus. World Heal. Organ., pp. 1–9

Yan, Z., Zhou, Y., Zhang, Y., Zhang, X., 2023. Distribution, bioaccumulation, and risks of pharmaceutical metabolites and their parents: a case study in an Yunliang River, Nanjing City. Int. J. Environ. Res. Public Health 20. https://doi.org/10.3390/ijerph20042967.

Zhang, Q., Huang, W., Hong, J. min, Chen, B.Y., 2018. Deciphering acetaminophen electrical catalytic degradation using single-form S doped graphene/Pt/TiO2. Chem. Eng. J. 343, 662–675. https://doi.org/10.1016/j.cej.2018.02.089.

Zhu, J., Wei, Z., Suryavanshi, M., Chen, X., Xia, Q., Jiang, J., Ayodele, O., Bradbury, B.D., Brooks, C., Brown, C.A., Cheng, A., Critchlow, C.W., Devercelli, G., Gandhi, V., Gondek, K., Londhe, A.A., Ma, J., Jonsson-Funk, M., Keenan, H.A., Manne, S., Ren, K., Sanders, L., Yu, P., Zhang, J., Zhou, L., Bao, Y., 2021. Characteristics and outcomes of hospitalised adults with COVID-19 in a Global Health Research Network: a cohort study. BMJ Open 11. https://doi.org/10.1136/bmjopen-2021-051588.